ELSEVIER

Journal of Hydrology 254 (2001) 124–144

Journal of Hydrology

www.elsevier.com/locate/jhydrol

Vegetation influence on runoff and sediment yield in the Andes region: observation and modelling

I. Braud[a,*], A.I.J. Vich[b], J. Zuluaga[c], L. Fornero[c], A. Pedrani[b]

[a]*LTHE (UMR 5564 CNRS, INP Grenoble, IRD, UJF), BP 53, 38041 Grenoble Cédex 9, France.*
[b]*IANIGLA/CONICET, Casilla de Correo 330, 5500 Mendoza, Argentina*
[c]*INA-CRA, Casilla de Correo 6, 5500 Mendoza, Argentina*

Received 13 July 2000; revised 23 April 2001; accepted 7 July 2001

Abstract

The Precordillera of the Andes Mountains (Mendoza, Argentina) is prone to severe flash floods, caused by heavy rainfall events of short duration and high intensities. Two catchments were instrumented in order to study the rainfall–runoff process and soil management impact on runoff and/or sediment yield. In the first catchment (Divisadero Largo, DL, 5.47 km^2), characterized by a large heterogeneity of surface geology, a data set of about 50 rainfall–runoff events covering the 1983–1994 period was available. Vegetation cover changed significantly after the catchment was enclosed in 1989–1990. This change was successfully mapped using Landsat TM image analysis. The second catchment (Cuenca Aluvional Piloto, CAP, 35 ha), the soil of which was homogeneous, was instrumented in 1992 for total runoff and sediment yield measurements. Three small plots of 3×10 m^2 (bare soil, 42 and 60% vegetation cover) and three sub catchments (2–4.5 ha) were delimited with different average vegetation cover. Data analysis showed the difficulty in relating runoff volume and sediment yield to simple descriptors of the catchments such as the average slope and/or the average vegetation cover. The DL and CAP catchments were modelled using the Areal Non Point Source Watershed Environment Response Simulation (ANSWERS) model with contrasting results. Good agreement between model and observation could be achieved after calibration on the 3×10 m^2 plots, but the model failed to correctly reproduce runoff on the three 2–4.5 ha CAP sub-catchments using the values calibrated on the small plots. Better results were obtained on the larger and heterogeneous DL basin, where surface geology variations and rainfall variability seemed to be the most influential factors. In this case, no sensitivity to vegetation coverage changes, induced when enclosing the catchment, was found. On the other hand, the model proved sensitive to differences in vegetation cover at smaller scales when the geology was homogeneous.

Keywords: Runoff; Sediment; Vegetation; Landsat TM images; Distributed model; Andes

1. Introduction

The Piemont and Precordillera areas of the Andes mountains situated in western Mendoza (33–33.5°S, 68.8–69.1°W) (Argentina) are prone to heavy summer rainfall events of short duration and high intensities, characterized by a large spatial and temporal variability over short distances (Fernández et al., 1999). These events can generate severe flash floods, dangerous for the downstream city of Mendoza.

A telemetric network of automatic rain gauges was

* Corresponding author. Tel.: 33-4-7682-5285; fax: 33-4-7682-5286.
E-mail address: isabelle.braud@hmg.inpg.fr (I. Braud).

0022-1694/01/$ - see front matter
PII: S0022-1694(01)00500-5

set up in 1983 on a study area of about 600 km^2, westward of the city of Mendoza (Fernández et al., 1988). A small catchment (Divisadero Largo, DL, 5.47 km^2) was also equipped for streamflow measurements. The aim was a better understanding of the rainfall–runoff process in the region. Another catchment (Cuenca Aluvional Piloto, CAP, 35 ha) was also instrumented in order to assess various management practices on runoff and sediment yield.

Data collected on the DL catchment were used in various rainfall–runoff studies using event-based models. The major drawback of these models is the specification of the initial soil moisture status of the catchment. Braud et al. (1999) successfully used the continuous version of the ANSWERS model (Beasley et al., 1980) proposed by Bouraoui and Dillaha, (1996) to avoid this problem. In this first study, vegetation cover was assumed constant in time. However, when the catchment was enclosed and became a natural reserve, vegetation cover increased significantly. Vegetation cover influence on the catchment response had to be studied in order to assess if the severity of flash floods and sediment yield could be limited by an increase in vegetation cover.

The CAP catchment data had been used to test and calibrate standard sediments yield models such as the USLE equation (Vich et al., 1998). Rainfall simulator infiltration tests were modelled using simple infiltration models (Nave, 1996; Vich and Nave, 1998). However, the data set had not been used to model the whole hydrological cycle and the sediment yield in relation with the vegetation coverage.

The aim of the present study were (i) to propose a method to assess vegetation cover changes from remote sensing (annual and long term evolution) and take it into account in the ANSWERS modelling framework (DL catchment) and (ii) propose a modelling of the rainfall–runoff–sediment yield processes on the CAP catchment, taking into account different vegetation cover. Given the satisfying results obtained on the DL catchment, the same ANSWERS model was also tested on the CAP catchment (three small plots of 30 m^2 and three sub catchments of 2–4.5 ha). Additionally, the study allowed to test the applicability (and transferability) of the same model across scales under a natural environment.

2. Material and methods

2.1. Model description

The original ANSWERS model, proposed by Beasley et al. (1980) was an event-based rainfall–runoff model. Bouraoui and Dillaha (1996) proposed a continuous version, where the evaporation process was included, allowing the model to be run continuously. This last version, restricted to water transfer only, was used in a first modelling work performed on the DL catchment (Braud et al., 1999). The sediment transport module, proposed by Beasley et al. (1980) was incorporated for the modelling work performed on the CAP catchment.

The following processes are represented in the model. After rainfall begins, precipitation can be intercepted by the canopy, until the interception capacity is exceeded. Then, throughfall can infiltrate into the soil, following the Green and Ampt (1911) model. When the infiltration capacity is exceeded (Horton, 1940) or the soil reservoir is saturated (saturation excess), water can accumulate at the soil surface into micro depressions. Once their storage capacity is exceeded, surface overland flow—modelled as a homogeneous sheet of water moving over a plane—can begin. Excess water is transferred to the channel and routed to the outlet (Bras, 1990). Water in excess of field capacity can drain to the groundwater when it is present. If the subsoil is impervious, the soil reservoir is progressively filled until saturation. During interstorm, water is allowed to evaporate from the soil surface or to be transpired by the plants (Ritchie, 1972).

The sediment transport module simulates detachment and transport up to 10 particle size classes. Soil particles can be detached both by rainfall impact and flow (shear stress and lift forces generated by overland flow). Both types of particles can be transported by overland flow, provided that enough energy is available to transport them. Otherwise, particles are deposited.

Detachment of soil particles by raindrop impact is calculated using the relationship described by Meyer and Wischmeier (1969):

$$DETR = CE1 \times CDR \times SKDR \times A_i \times R^2 \quad (1)$$

where $DETR$ (kg s^{-1}) is the rainfall detachment rate,

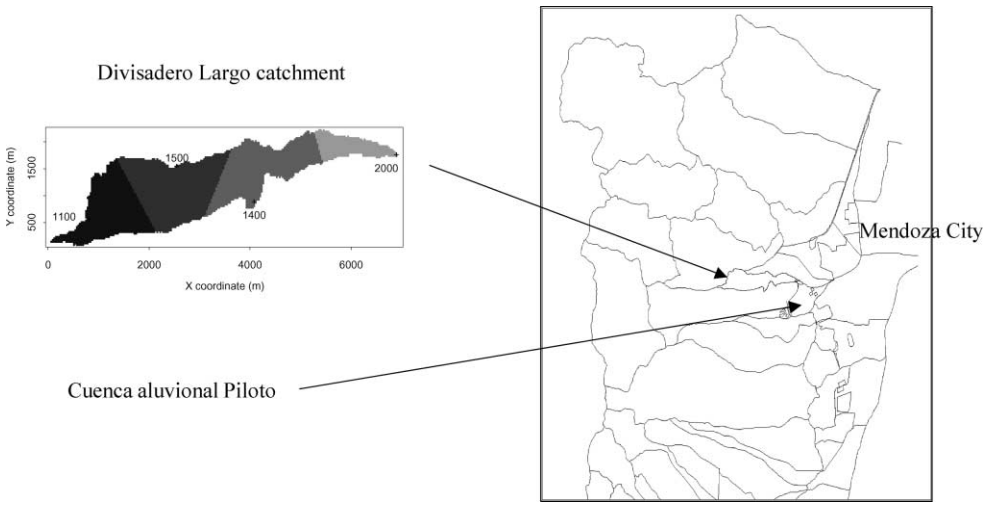

Fig. 1. Location of the study area, in the Mendoza province, Argentina.

CDR is the cropping and management factor *C* (from Universal Soil Loss Equation—Wischmeier and Smith, 1978), *SKDR* is the soil erosivity factor *K* (from Universal Soil Loss Equation), A_i (m^2) is the area increment and *R* ($m\ s^{-1}$) is the rainfall intensity. *CE*1 is a constant with a default value of 6.54×10^6 (Bouraoui, 1994).

The detachment of soil particles by overland flow was described by Meyer and Wischmeier (1969) and modified by Foster (1976) as follows:

$$DETF = CE2 \times CDR \times SKDR \times A_i \times SL \times Q \qquad (2)$$

where *DETF* ($kg\ s^{-1}$) is overland flow detachment rate, *SL* is the slope steepness (%) and *Q* is the flow per unit width ($m^2\ s^{-1}$). *CE*2 is a constant with a default value of 52.5 (Bouraoui, 1994).

Both *CE*1 and *CE*2 can be considered as adjustable constants. Detachment and transport are calculated for various particle classes according to the particle size distribution of the sediments. Yalin's equations (1963) as extended by Mantz (1977) for small particles are used to calculate actual transport capacity for each particle. Details can be found in Beasley et al. (1980); Bouraoui et al. (2000).

ANSWERS is a distributed model, where the catchment is represented as a set of square grid elements, over which properties are assumed to be uniform. However, the model can take into account variations of topography, soil type, vegetation cover and land use across the catchment. The time evolution of vegetation cover and land use can also be described. Rainfall spatial variability can be taken into account through Thiessen polygons, each grid cell being associated with one rainfall gauge.

2.2. Data available and data processing

Fig. 1 shows the localization of the catchments, within the pilot zone defined westward of the city of Mendoza, Argentina, near the Chilean border. The climate of the zone is arid with an average rainfall of 206 mm (Vich, 1996). Rainfall regime is characterized by summer events of low duration (a few hours), high intensities and small spatial extension (Fernández et al., 1999). Winter events are of larger spatial extension, but lead to low intensities. A telemetric rainfall network has been operating since 1983, providing rainfall intensities at about 25 gauges, with a time resolution all the more fine as the intensity is high (time of tipping of 1 mm auger capacity is recorded). Four rain gauges are situated within the DL catchment (stations 1100, 1400, 1500, 2000) and one gauge within the CAP catchment (station 2100). Their records could be directly used within the ANSWERS model, leading to a very fine time resolution during rainfall events.

Climatic data, including mean daily air temperature and incoming global radiation, as needed by the

Table 1
Available dates and channels of Landsat TM images

Dates	Channels[a,b]
22 February 1986	TM1, 2, 3, 4, 5, 6, 7
15 March 1988	TM1, 2, 3, 4, 5, 6, 7
7 September 1988	TM1, 2, 3, 4, 5, 6, 7
20 August 1993	TM3, 4, 5
5 December 1997	TM1, 2, 3, 4, 5, 6, 7

[a] The wavelengths corresponding to each channel are the following: visible: TM1 (0.45–0.52 μm); TM2 (0.52–0.60 μm); and TM3 (0.63–0.69 μm), infra-red and near-infra red: TM4 (0.76–0.90 μm); TM5 (1.55–1.75 μm); and TM7 (2.08–2.35 μm) and thermal: TM6 (10.4–12.5 μm).

[b] The pixel size is 30×30 m2, except for the thermal channel (TM6) which has a degraded resolution (120×120 m^2).

model to compute potential evaporation, were obtained from the Mendoza airport meteorological station (information obtained from SMN-INTA and J. Morabito INA-CRA) representative of desert conditions.

2.2.1. Divisadero Largo

The catchment is 5.47 km^2 (7 km long and 1.5 km wide), with relatively high slopes (the outlet altitude is 950 m and the highest point within the catchment is 1420 m high). Surface geology is complex, including eight formations, six of which covering 23% of the surface, can be considered as quasi-impervious. Soil thickness is very low (from a few centimetres to about 1 m), with high coarse fragments of about 40% except the Marine formation (10%). Vegetation is sparse and dominated by shrubs less than 2 m height. In 1989–1990, the catchment was enclosed to avoid cattle grazing and was transformed into a natural reserve. Since this date, an understorey of gramineas has grown up, increasing the vegetation cover.

About 50 rainfall–runoff events collected between 1983 and 1994, including rainfall and streamflow time series were available for model evaluation. However, as the river was dry most of the time, problems with the streamflow sensor were encountered, reducing the quality of the data, especially for the last years. It was, therefore, not possible to assess possible decrease of runoff production after closure of the catchment from data analysis only.

The derivation of input data maps, as needed by the ANSWERS model was described in Braud et al. (1999). A topography map with a 30 m resolution (also the resolution of the model grid cell) was used to derive the channel network and the slope map, using the PC RASTER Package (Van Deursen and Wesseling, 1992). Six soil classes were defined from the geological map and the soil hydrodynamic properties defined from in situ and laboratory measurements (Ligtenberg et al., 1992) and used in ANSWERS. In this first study, a vegetation map was derived (four classes according to the vegetation cover) from a Landsat TM image of 22 February 1986, i.e. before the catchment was enclosed. Finally, a surface storage capacity map was derived by combining this vegetation map and the slope map, according to FAO standard.

In the present study, additional Landsat TM images were processed using the IDRISI software (Eastman, 1995) in order to define the annual and long term evolution of vegetation cover. Given problems encountered in reading old magnetic tapes, only five images were finally available. The corresponding dates and channels are given in Table 1. Radiometric corrections, accounting for the sun position and the date within the year, were performed in order to get comparable reflectances for the various dates. Previous studies (Zuluaga et al., 1988) had shown that the atmosphere of the region was pure enough to neglect atmospheric corrections, which were not performed. All the maps were geo-referenced in the same co-ordinate system (Braud, 1999). The Normalized Difference Vegetation Index (*NDVI*) was calculated using Eq. (3).

$$NDVI = \frac{TM4 - TM3}{TM4 + TM3} 100 \tag{3}$$

A previous study (Roby et al., 1988), combining Landsat TM image analysis and in situ sampling led to a relationship between *NDVI* and vegetation coverage V_{eg} (%). This relationship was adapted to account for very low and negative values of *NDVI* associated with a high reflectivity of bare soil, when vegetation cover is low.

$$V_{eg} = \begin{cases} 0 & NDVI < 0 \\ 0.4125NDVI & 0 \le NDVI \le 16 \\ 2.64(NDVI - 13.5) & NDVI \ge 16 \end{cases} \tag{4}$$

This relationship was assumed to be valid for all the

Table 2
Statistics of vegetation coverage (%) maps of the Divisadero Largo catchment

Date	Minimum	Maximum	Average	Standard deviation
22 February 1986	0	83.2	31.8	11.9
15 March 1988	0	70.0	13.7	9.4
7 September 1988	0	43.6	5.0	2.7
20 August 1993	0	51.5	8.2	5.7
5 December 1997	0	78.8	34.8	8.7

images, due to the absence of new coincident image and in situ sampling. Obtained results (see Table 2) were consistent with expectation, showing that Landsat TM images can be used successfully to describe vegetation time evolution. Winter images from September 1988 and August 1993 can be considered as representative of the lowest vegetation cover of the year. This minimum value is higher in 1993 as expected after the closure of the catchment in 1989–1990. Average values of February 1986 and December 1997 summer images were very close. However, in 1986, this value was the maximum vegetation cover, whereas in 1997, the growing phase of the vegetation had just begun. Fig. 2 shows vegetation cover for February 1986 and December 1997. It can be seen that regions of very low vegetation cover in 1986, situated in the middle of the catchment, had been significantly re-vegetated.

Average vegetation cover of March 1988 summer image is much lower than that of February 1986, an effect of the interannual variability of rainfall regime. Indeed, between November 1985 and 22 February 1986, the cumulative rainfall was 164 mm, whereas it was only half this value (83 mm) between November 1987 and 22 February 1988. About 38 mm additional rainfall fell between 22 February 1988 and 15 March 1988, but this was probably insufficient to compensate a lower vegetation development in the first part of the growing season. These continuous maps were transformed into vegetation classes, according to cuttings in the histograms (Braud, 1999)

As input for the ANSWERS model, three parameter files were prepared, each one being characterized by a typical Leaf Area Index evolution and a surface storage capacity map (Braud, 1999), representative of the 1983–1990 (before the closure), 1990–1993 (growing phase of the vegetation), 1994–1998 (supposed to be another stable state), because the small number of available images did not allow for a more precise description. These parameter files were used to assess vegetation influence on model outputs; namely runoff volume and peak discharge.

2.2.2. Cuenca Aluvional Piloto

The Cuenca Aluvional Piloto (35 ha) catchment is situated westward of the city of Mendoza (32°52′50″S, 68° 52′00″W). Within this catchment, three small fields, denoted CAP1, CAP2 and CAP3, of $3 \times 10\ m^2$ and three sub-catchments (Jarillal, Grande and Garabato) were instrumented. Their main characteristics are summarized in Table 3. The three small plots could be considered as uniform in slope and vegetation cover (Tables 3 and 4). They were discretized as shown in Fig. 3.

For the three subcatchments, in situ measurements of the height above see level were available on a $5 \times 5\ m^2$ grid. As for the DL catchment, the PC RASTER package (Van Deursen and Wesseling, 1992) was used to compute the slope map (see Fig. 4 for the maps and Fig. 5 for the histograms) and the drainage network. Vegetation cover maps were derived from in situ field survey. Two main vegetation covers were found for each subcatchment (Table 4 and Fig. 4). The surface storage capacity was defined according to Table 5. The geology of the catchment was uniform, contrarily to the DL catchment, with only one surface formation (Mogotes). Its hydraulic characteristics have been published by Nave (1996); Vich et al. (1998); Vich and Nave (1998) and were derived from in situ rainfall simulator infiltration tests on a $50\ m^2$ area. They are summarized in Tables 6 and 7. Another soil type, representing impervious zones was also defined for the three subcatchments (see Section 3.2).

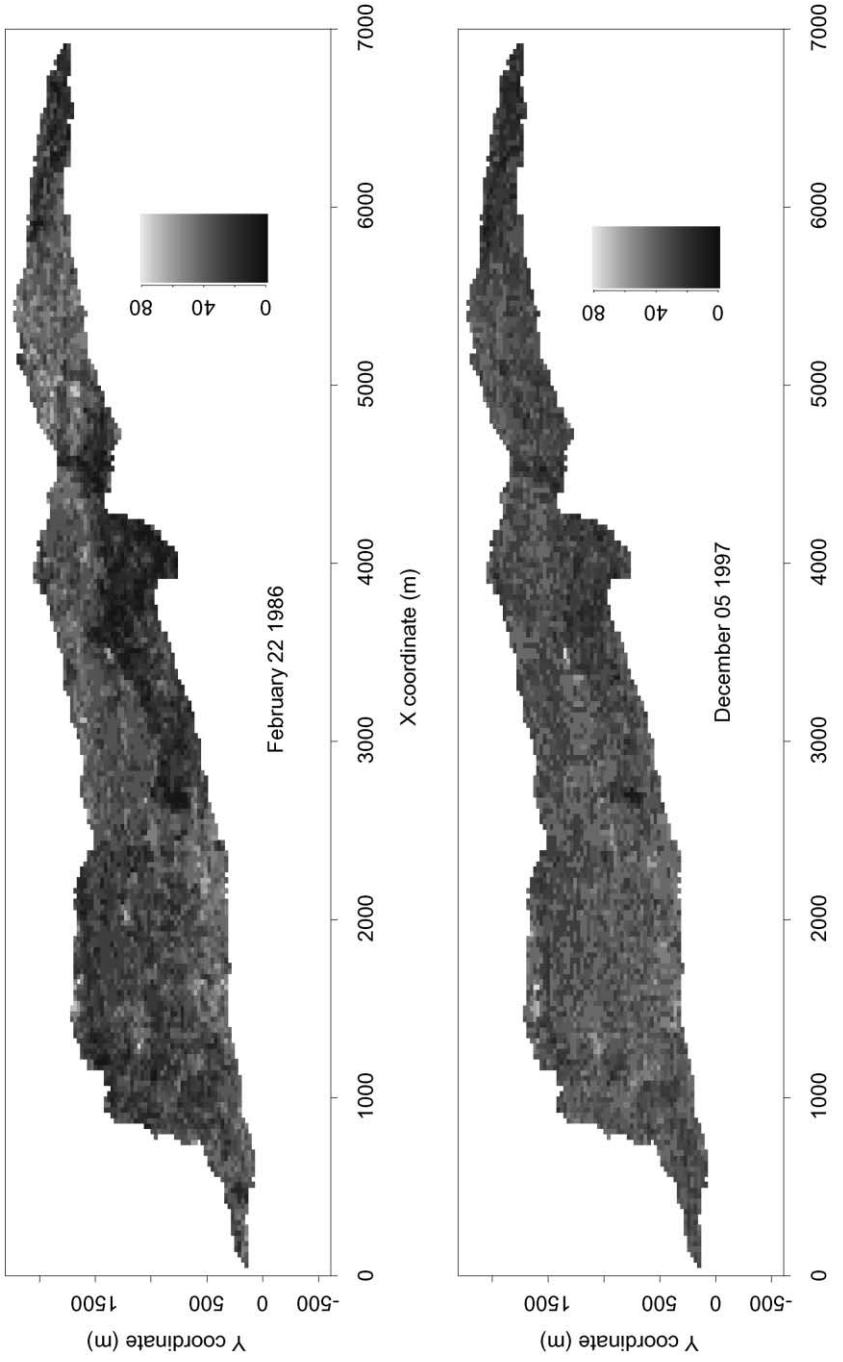

Fig. 2. Vegetation cover (%) maps of the Divisadero Largo catchment for two dates: 26 February 1986 (top) and 5 December 1997 (bottom).

Table 3
General catchments characteristics within the Cuenca Aluvional Piloto catchment

Catchment	Surface (m^2)	Average slope (%)	Pixel size (m)	Element numbers	Channel flow element number
CAP1	30	19.6	1	30	0
CAP2	30	16.7	1	30	0
CAP3	30	14.6	1	30	0
Grand	3050	40.4	5	122	29
Jarillal	1975	28.6	5	79	23
Garabato	4525	16.5	5	181	49

2.3. Assessment of model performance and simulation carried out

Parameter files described previously were used as input of the ANSWERS model. In the DL catchment, four rain gauges were used and rainfall spatial variability could be taken into account. Simulations were performed from 1983 to 1997. On the CAP catchment, the model was applied to the three small plots ($3 \times 10\ m^2$) and the three sub catchments presenting various vegetation cover from 1987 to 1998.

The following statistical criteria were used to quantify model performance:

Average bias B:

$$B = \frac{1}{n}\sum_{i=1}^{n}(Y_{i\mathrm{bmod}} - Y_{i\mathrm{obs}}) \tag{5}$$

Efficiency E:

$$E = 1 - \frac{\sum_{i=1}^{n}(Y_{i\mathrm{bmod}} - Y_{i\mathrm{obs}})^2}{\sum_{i=1}^{n}(Y_{i\mathrm{bmod}} - \bar{Y}_{i\mathrm{obs}})^2} \tag{6}$$

Root Mean Square Error $RMSE$:

$$RMSE = \sqrt{\frac{1}{n}\sum_{i=1}^{n}(Y_{i\mathrm{bmod}} - Y_{i\mathrm{obs}})^2} \tag{7}$$

Mean Absolute Error MAE:

$$MAE = \frac{1}{n}\sum_{i=1}^{n}|Y_{i\mathrm{bmod}} - Y_{i\mathrm{obs}}| \tag{8}$$

where n is the number of data, $Y_{i\mathrm{mod}}$ and $Y_{i\mathrm{obs}}$ are the calculated and observed variables and $\bar{Y}_{\mathrm{obs}}$ is the average of the observations. Regressions between observed and calculated values were also estimated: $Y_{i\mathrm{bmod}} = Slope^{*}Y_{i\mathrm{obs}} + Intercept$ with coefficient of determination R^2.

For the CAP catchment, B, E and $RMSE$ were evaluated on total runoff and sediment yield. The samples size (14–16 events) was not large enough to allow for the definition of independent calibration and validation samples. Therefore, five events were drawn randomly within each sample and kept apart for model validation (in order to get statistically significant results, what is called validation sample in the following was composed of the calibration sample plus the five validation events).

For the DL catchment, year 1985 had been used for model calibration and the 33 events available on the 1983–1994 period used for model validation (Braud et al., 1999), using all the above mentioned statistical criteria calculated on total runoff and peak discharge.

3. Analysis of runoff and sediment yield data within the CAP catchment

3.1. Results

A first step was to compare behaviours between the smaller and larger scales. Table 8 shows statistics calculated on the runoff coefficient RC (defined as the ratio of runoff over rainfall), runoff volume and sediment yield for the three small plots and sub catchments. Runoff coefficients of the small plots were high. CAP1 field average value reached 0.44. It was 0.34 for the CAP2 field (60% vegetation cover) and 0.22 for the CAP3 field (42% vegetation cover). On the other hand, average runoff coefficients never

Table 4
Characteristics of the vegetation types defined within the Cuenca Aluvional Piloto catchment

Vegetation type	Measures					ANSWERS parameters			
	Average cover (%)	Covered surface (%)	Surface stone content (%)[a]	Litter fraction (%)[a]	Shrubs fraction (%)[b]	Leaf area index	Potential interception (mm)	Manning coefficient for overland flow	Surface storage capacity (mm)
CAP1	0	100	–	–	–	0	0.00	0.01	1.0
CAP2	60	100	–	–	–	1.83	0.22	0.07	1.0
CAP3	42	100	–	–	–	1.08	0.09	0.05	2.0
Grande Type 1	64	67	20	4	50	2.04	0.26	0.09	Table 5
Grande Type 2	50	33	17	7	32	1.39	0.14	0.07	Table 5
Jarillal Type 1	75	62	13	3	71	2.77	0.41	0.09	Table 5
Jarillal Type 2	52	38	24	10	31	1.47	0.15	0.07	Table 5
Garabato Type 1	50	76	31	7	27	1.39	0.14	0.07	Table 5
Garabato Type 2	86	24	6	1	80	3.93	0.67	0.10	Table 5

[a] Fraction of the surface covered by the vegetation type.
[b] Fraction of the vegetated surface.

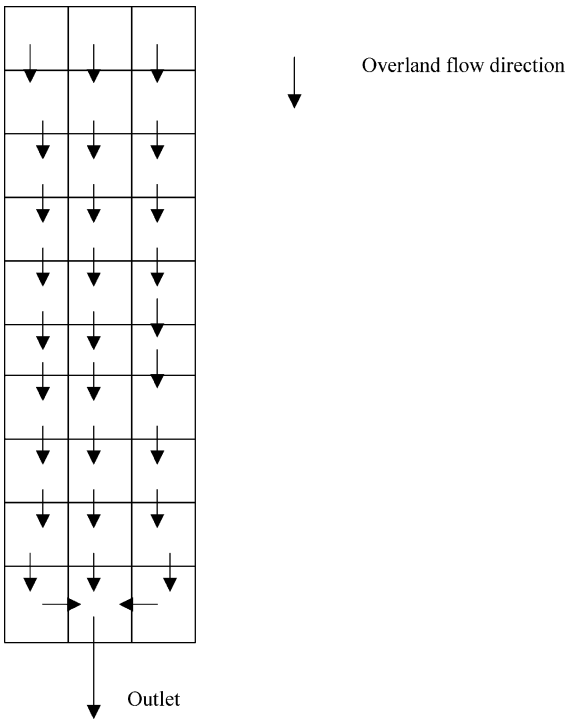

Fig. 3. Discretization scheme of the small rectangular fields with the flow direction.

exceed 0.09 on the three sub-catchments showing a dramatic decrease when moving from the small scale (30 m^2) to the medium scale (2000–5000 m^2). Furthermore, data analysis (Braud, 1999) showed that, for the three small fields, runoff production was associated with rainfall higher than 11–13 mm. On the other hand, runoff could occur on the three sub-catchments with total rainfall as low as 2–10 mm. Associated runoff coefficients were lower than 0.01, but this observation shows behavioural differences in runoff appearance when moving form the smaller to the larger scales.

The second step of the analysis was to seek for relationships between runoff and sediment yield and vegetation cover. Figs. 6 and 7 show the comparison of runoff volume between the three small plots and the three sub catchments respectively. Vegetation influence could clearly be seen on the three small fields. Indeed, bare soil (CAP1) runoff and sediment yield were almost always higher than for the vegetated surfaces (Tables 6 and 7) as expected. However, runoff and sediment yield were in general higher (especially for larger events) for the 60% coverage (CAP2) than for the 42% coverage field (CAP3). The slope of the 60% coverage field was higher

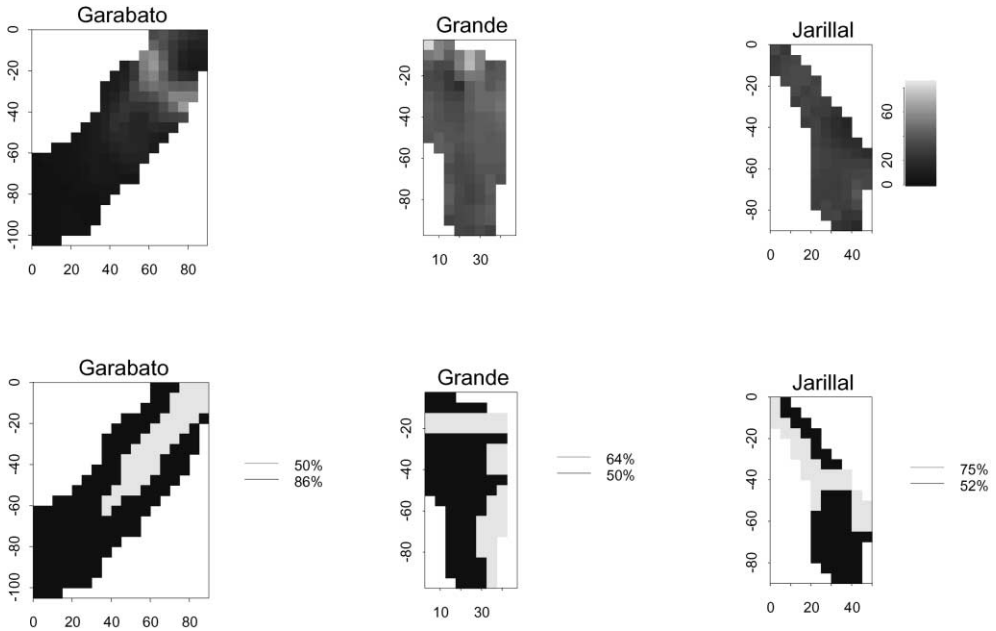

Fig. 4. Slope maps (%) (top panel) and vegetation maps (bottom panel) for the Garabato (left), Grande (middle) and Jarillal (right) catchments.

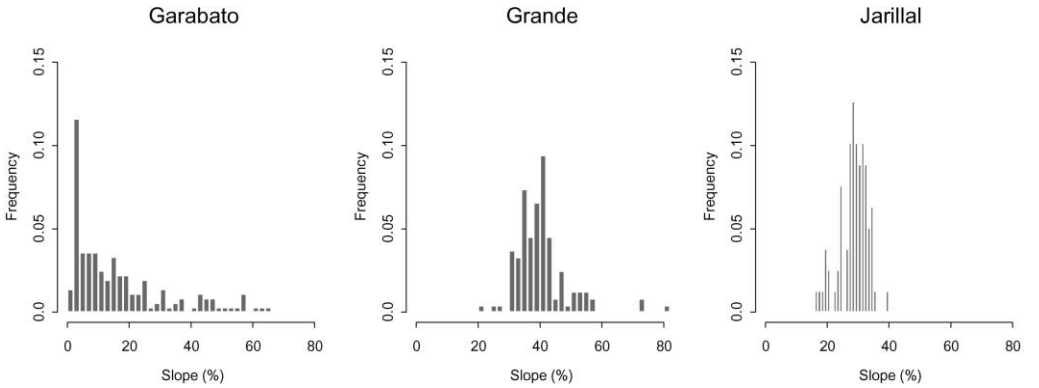

Fig. 5. Slope histograms (%) for the Garabato (left), Grande (middle) and Jarillal (right) catchments.

(16.7% rather than 14.6%), but the result was unexpected. For sediment yield, bare soil production was much higher than that of vegetated surfaces. On the other hand, although runoff of the CAP3 field was lower than that of the CAP2 field, they exhibited similar sediments yields.

When comparing the three sub-catchments, the interpretation of the results was less obvious. Table 8 and Fig. 7 show that runoff of the Grande catchment was lower than that of the other two. Garabato catchment average runoff coefficient was lower than that of the Jarillal catchment, but Fig. 7 shows that it was sometimes higher and sometimes lower. The average runoff coefficient was the highest for the catchment with the smallest area (1975 m^2) and the intermediate average slope (28.7%). The Grande catchment exhibited the lowest average runoff coefficient, but the highest average slope and the lowest vegetation coverage (see Table 4). Table 8 shows that there was no link between runoff production and sediment yield on the sub catchments. Indeed, the Grande catchment exhibited a sediment yield much lower than the Jarillal one, although their average runoff was similar and although the Grande catchment slope was higher than that of the Jarillal catchment. The Garabato catchment produced the lowest sediment yield, but it was the second in runoff production. This catchment exhibited the highest vegetation coverage and lowest average slope.

3.2. Discussion

A dramatic decrease in runoff coefficients when moving from the small scale (30 m^2) to the medium scale (2000–5000 m^2) was observed. As the slope of the sub-catchments was in general higher than that of the small fields, that the soil and vegetation were similar, it must be recognized that new phenomena are probably activated when moving to largest scales. One explanation might be found in different surface storage capacities linked to differences in micro-topography. Indeed, the three small plots were levelled and chosen so that the slope was uniform. On the other hand, under natural conditions, micro depressions, big stones are more common and could retain more water than on the small fields. The decrease of runoff when

Table 5
Surface storage capacity (mm) for the three sub-catchments

Surface storage capacity	Slope (%)	Grande		Jarillal		Garabato	
		Type 1 64%	Type 2 50%	Type 1 75%	Type 2 52%	Type 1 50%	Type 2 86%
Very low	> 30%	9	5	6	6	9	7
Low	15–30%	7	4	5	5	7	5
Medium	10–15%	5	3	4	4	5	2
High	0–10%	3	2	3	3	3	1

Table 6

Table 6.a: Characteristics of the soil types (one type for the three small plots and two types for the three sub-catchments).

	CAP1	*CAP2*	*CAP3*	*Grande*	*Jarillal*	*Garabato*
Depth (mm) (*)	20 -	30 -	40 -	150 20	40 20	120 20
Total porosity (-)	0.47 -			0.47 0.47		
Fraction of coarse fragments (%)	45.3 -			45.3 45.3		
Field capacity (fraction of saturation)	0.80 -			0.80 0.80		
Wilting point (fraction of saturation)	0.20 -			0.20 0.20		
Saturated hydraulic conductivity (mm hr^{-1}) (*)	19 -	16 -	7 -	8 0.05	16 0.05	16 0.05
Wetting front suction (cm)	0.12 -			0.12 0.12		
Coefficient *C* of the USLE	0.03	0.02	0.03	0.03	0.03	0.03
Coefficient *K* of the USLE	0.27			0.27		
Coefficient *CE1* (*) (**)	30**CE1*	4.5**CE1*	4.5**CE1*	4.5**CE1*	4.5**CE1*	4.5**CE1*
Coefficient *CE2* (*) (**)	10**CE2*	5**CE2*	5**CE2*	5**CE2*	5**CE2*	5**CE2*

(*) Calibrated values
(**) Reference values are *CE1*=6.54 10^6 and *CE2*=52.5

Table 6.b: Texture of the Mogotes formation.

Particle diameter	<0.002 mm	0.002-0.01 mm	0.01-0.05 mm	0.05-2 mm	> 2 mm
Percentage	0.8	10	15	74.2	45.3
Specific gravity	2.65	2.65	2.65	2.65	-
Equivalent sand diameter (mm)	0.002	0.01	0.05	2	-
Fall velocity (m s^{-1})	0.0000036	0.0000896	0.00215	0.2921	-

moving from smaller to larger scales was also reported by other authors, e.g. Descroix and Nouvelot (1997) in La Sierra Madre, Mexico; Bergkamp (1998) in Castilla La Mancha, Spain. Bergkamp (1998) explained this decrease in runoff production by the absence of connection between runoff production zones, and a partial downslope re-infiltration of the runoff.

The rainfall threshold leading to the production of runoff was found to be much smaller for the medium scale than for the small scale. The runoff produced for small rainfall amounts in the sub catchments could be associated with the existence of quasi-impervious zones very close to the channel outlet (presence of big stones within the riverbed near the outlet). If we assume that the average runoff coefficient associated with these low rainfall events was representative of the impervious area, we get 0.4% of the catchment for the Jarillal catchment (7.9 m^2), 0.083% for the Garabato catchment (3.7 m^2) and 0.23% for the Grande catchment (7 m^2). This area represents less than a pixel of the ANSWERS model (25 m^2). This observation justifies the adjunction of a second soil type with a low hydraulic conductivity, in the modelling of the three sub-catchments (see Tables 6 and 7). This low value was assumed identical to that of the quasi-impervious soil type of the DL catchment (Braud et al., 1999). Only one pixel (the outlet) was assigned to

Table 7
Texture of the Mogotes formation

Particle diameter	< 0.002 mm	0.002–0.01 mm	0.01–0.05 mm	0.05–2 mm	> 2 mm
Percentage	0.8	10	15	74.2	45.3
Specific gravity	2.65	2.65	2.65	2.65	–
Equivalent sand diameter (mm)	0.02	0.01	0.05	2	–
Fall velocity (m s^{-}1)	0.0000036	0.0000896	0.00215	0.2921	–

Table 8
Statistics of runoff coefficient RC and sediment yield for the three small plots and the three subcatchments

	CAP1	CAP2	CAP3	Garabato	Jarillal	Grande
	Runoff coefficient RC (–)					
Minimum	0.07	0.08	0.01	0.0003	0.0032	0.0005
Maximum	0.91	0.76	0.45	0.0454	0.0851	0.0274
Average	0.44	0.34	0.22	0.013	0.021	0.009
Standard deviation	0.24	0.21	0.13	0.017	0.020	0.010
	Runoff volume (mm)					
Minimum	1.9	2.1	0.2	0.002	0.01	0.004
Maximum	35.9	35.6	17.4	1.25	1.78	0.79
Average	11.7	9.8	5.5	0.27	0.41	0.17
Standard deviation	10.8	10.0	5.2	0.36	0.56	0.25
	Sediment yield (kg ha^{-}1)					
Minimum	70.4	37.5	0.035	0.0013	0.0046	0.0031
Maximum	7950.2	1874.9	1090.0	44.9	628.4	23.5
Average	1451.7	379.1	187.6	7.2	45.4	4.9
Standard deviation	2286.1	572.1	314.0	12.5	151.2	7.8

this second soil type in the modelling work discussed in the next section. This allowed the model to predict a small runoff, even for low rainfall events. It was not the case when only one uniform soil type was used. However, the appearance of runoff even for small rainfall amounts (in general associated with previous rainfall events not producing runoff) could be the signature of preferential flows produced by macropores, roots, or microtopography channelling water movement (Estèves et al., 2000). The latter process

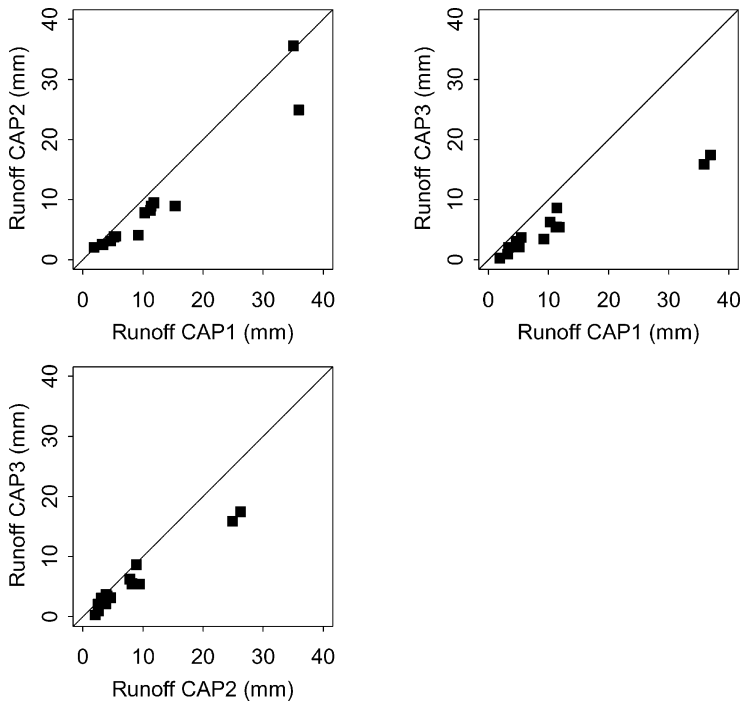

Fig. 6. Comparison of measured total runoff over the three small plots.

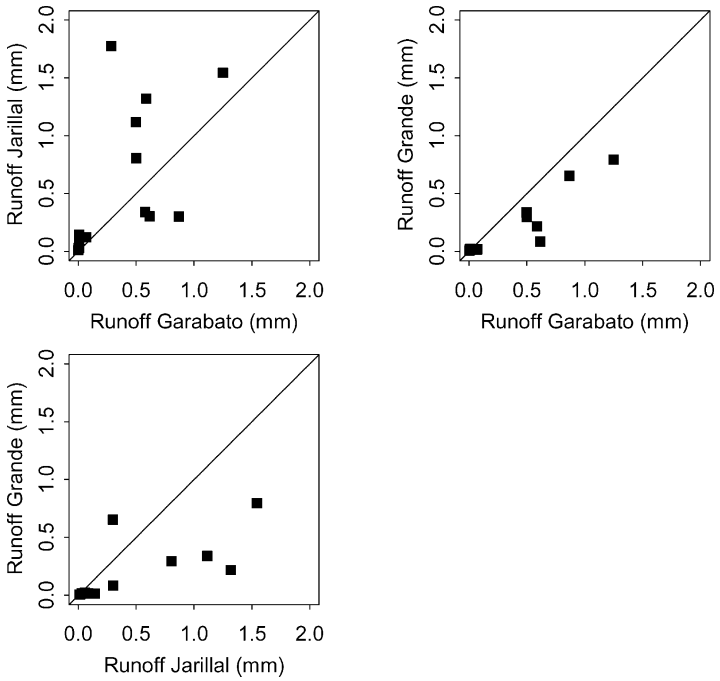

Fig. 7. Comparison of measured total runoff over the three subcatchments.

could have disappeared on the small plots when setting up the measurement devices. Preferential flow is not taken into account in the ANSWERS model, where runoff is assumed to move uniformly on a plane sheet.

This first analysis showed the difficulty to directly relate runoff and sediment yield with the average catchment characteristics such as slope or vegetation, even if the relationship was more direct for the small plots. As mentioned before, this difficulty might reflect that average parameters are not sufficient to characterize runoff and sediment yield generation, when the soil type is identical. Differences in micro-topography, stone cover, shrubs species, presence of litter could be responsible for differences in response. However, the Grande and Jarillal catchments exhibit similar surface stone and litter contents. The Jarillal catchment exhibits a larger shrub fraction than the Grande catchment, a smaller average slope and similar slope histograms (Fig. 5) and the Jarillal catchment produces more than twice runoff and 10 times more sediment. This result is far from expected, but other studies led to such results (see Descroix et al., 2001 for a review). In their own study, they showed that stoniness could enhance runoff when the stones were embedded into the crusted soil, whereas when they were free, the soil was protected and runoff reduced. The information on stone status within the CAP catchment is lacking and should be collected in order to improve data analysis. Differences in shrub species could also explain differences in runoff prediction. Indeed, the Jarillal species, dominant in the Jarillal catchment has prickly whereas the dominant shrubs of the Grande catchment have larger leaves. Descroix et al. (2001) also reported a better protection induced by oaks than by coniferous. Differences in plants should also be investigated further in the CAP catchment in order to assess more efficient practices in reducing runoff and erosion.

4. Application of the ANSWERS model

4.1. Application of the ANSWERS model to the CAP1, CAP2 and CAP3 plots

In a first verification of model behaviour, it was intended to reproduce infiltration and runoff volumes

Table 9
Bias, efficiency and root mean square error calculated on the three small plots with the calibration and validation samples for total runoff volume. Averages and standard deviations of observed runoff volume appear in Table 8

Test[a]	Calibration			Validation		
	B	*E*	*RMSE*	*B*	*E*	*RMSE*
CAP1						
$DF = 150$ $KS = 22$	− 5.37	0.51	6.74	− 7.50	0.24	9.09
$DF = 20$ $KS = 19$	1.36	0.89	3.26	0.26	0.87	3.74
$DF = 100$ $KS = 3$	1.45	0.83	3.98	0.30	0.84	4.14
CAP2						
$DF = 150$ $KS = 16$	− 5.56	0.30	7.68	− 7.29	0.09	9.28
$DF = 30$ $KS = 16$	− 1.14	0.91	2.73	− 1.06	0.87	3.51
$DF = 150$ $KS = 7$	− 2.66	0.76	4.53	− 3.89	0.70	5.35
CAP3						
$DF = 150$ $KS = 16$	63.41	0.33	4.00	− 3.98	0.12	4.76
$DF = 40$ $KS = 16$	− 1.75	0.79	2.25	− 1.29	0.26	4.30
$DF = 150$ $KS = 7$	− 1.55	0.66	2.87	− 1.32	0.59	3.2

[a] *DF* is the soil depth (mm) and *KS* is the saturated hydraulic conductivity (mm h^{-1})

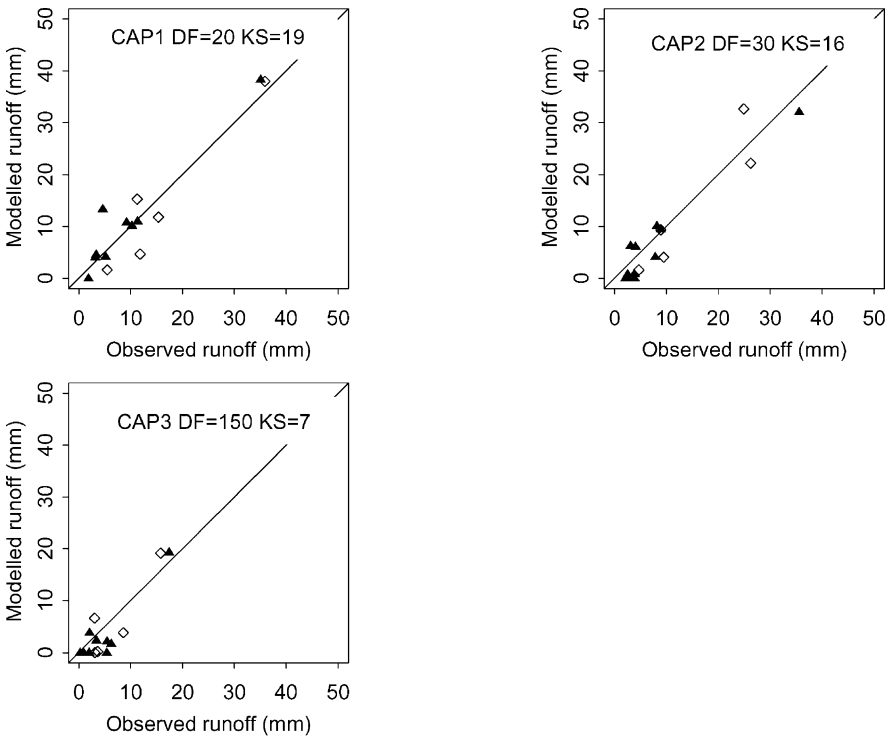

Fig. 8. Comparison of observed and calculated total runoff (mm) for the three small plots. Black points belong to the calibration set and white points are the validation events.

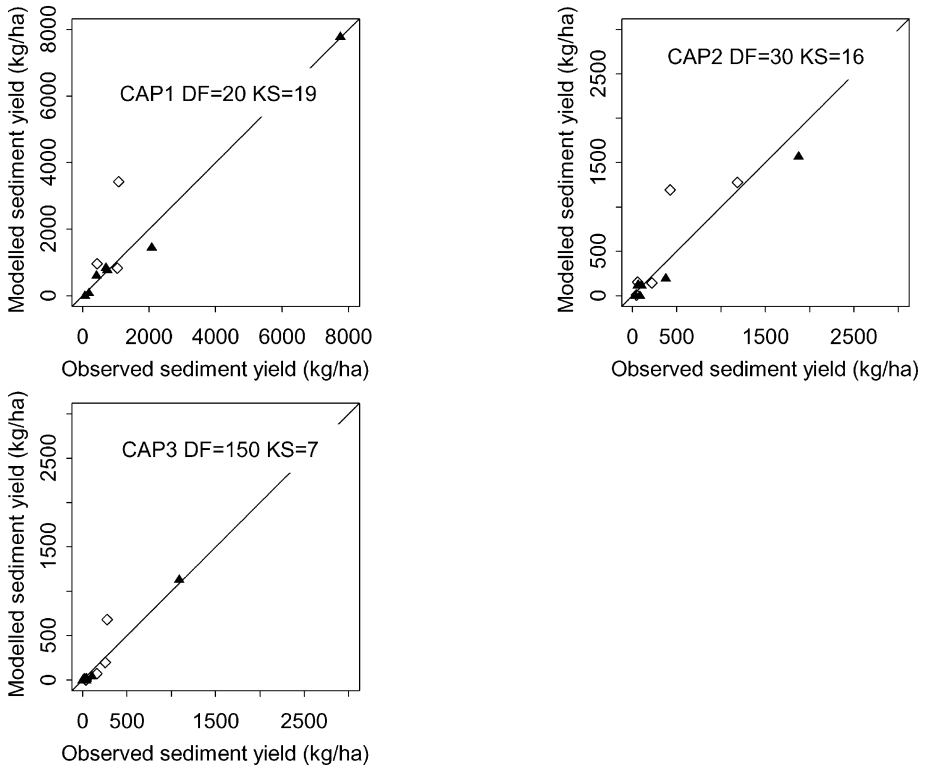

Fig. 9. Comparison of observed and calculated sediment yield (kg ha^{-1}) for the three small plots. Black points belong to the calibration set and white points are the validation events.

measured during infiltration tests performed with a 50 m^2 rainfall simulator. Good results were obtained with the saturated hydraulic conductivity, $KS = 28$ mm h^{-1}, reported by Vich and Nave (1998) and a 150 mm soil depth, *DF*. These values were then used on the three small plots, comparing model performance when the subsoil was supposed pervious or impervious. None of the cases led to good results (Table 9) and model calibration was needed, *DF* and *KS* being the adjustable parameters. Table 9 presents the most significant results. The best results were obtained when the subsoil was supposed to be pervious with, either a large soil depth *DF* associated with a *KS* one order of magnitude lower than that given by the rainfall simulator infiltration tests, or a *KS* corresponding to the rainfall simulator infiltration tests, but a very low soil depth *DF* (Table 9). Fig. 8 shows the correlation between calculated and observed runoff values for the three small plots and Fig. 9 the correlation between calculated and observed sediment yield, corresponding to the best validation results for runoff volume (Table 10). These results were obtained after adjusting the coefficients *CE*1 and *CE*2 (Tables 6 and 7), controlling detachment

Table 10
Bias, efficiency and root mean square error calculated on the three small plots with the calibration and validation samples for sediment yield. Averages and standard deviations of observed sediment yield appear in Table 8

Test[a]	Calibration			Validation		
	B	*E*	*RMSE*	*B*	*E*	*RMSE*
CAP1						
$DF = 20$ $KS = 19$	− 60.0	0.99	257.6	225.1	0.87	793.4
CAP2						
$DF = 30$ $KS = 16$	− 68.1	0.95	141.6	29.6	0.79	250.1
CAP3						
$DF = 150$ $KS = 7$	− 14.3	0.99	34.0	11.1	0.81	129.4

[a] *DF* is the soil depth (mm) and *KS* is the saturated hydraulic conductivity (mm h−1).

Table 11
Bias, efficiency and root mean square error calculated on the three subcatchments with the calibration and validation samples for total runoff volume. Averages and standard deviations of observed runoff volume appear in Table 8

Test[a]	Calibration			Validation		
	B	*E*	*RMSE*	*B*	*E*	*RMSE*
Jarillal						
$DF = 40$ $KS = 16$	− 0.03	0.39	0.42	0.57	− 25.0	2.83
Grande						
$DF = 150$ $KS = 8$	0.05	0.66	0.14	0.04	0.51	0.17
$DF = 150$ $KS = 16$	− 0.02	0.60	0.15	0.06	0.40	0.19
Garabato						
$DF = 150$ $KS = 16$	− 0.11	0.60	0.23	0.12	− 11.74	1.27
$DF = 120$ $KS = 16$	− 0.08	0.63	0.22	0.14	− 11.12	1.26

[a] *DF* is the soil depth (mm) and *KS* is the saturated hydraulic conductivity (mm $h^{-}1$).

by rainfall and by overland flow respectively, the first process appearing as the most important in the case study.

Finally, a simulation was performed in order to quantify model response to vegetation cover, using the same values, $DF = 150$ mm and $KS = 16$ mm h^{-1} for the three small plots. The largest runoff was calculated on the bare soil field (CAP1),

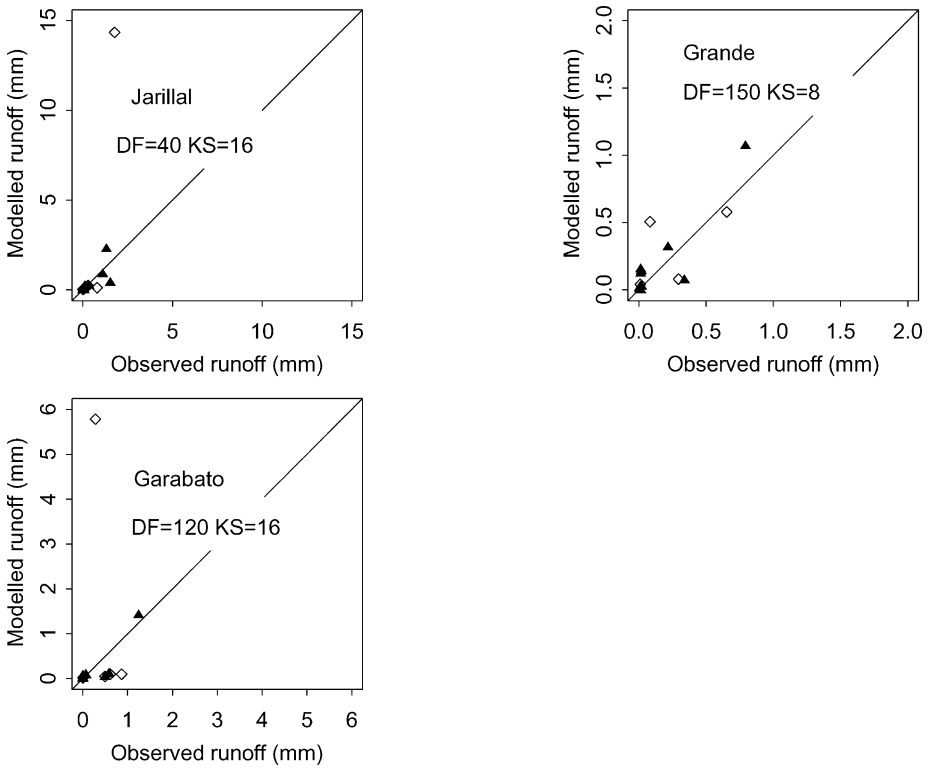

Fig. 10. Comparison of observed and calculated total runoff (mm) for the three subcatchments. Black points belong to the calibration set and white points are the validation events.

Table 12
Statistical comparison (calibration set) between observed and calculated runoff for the three sub-catchments when the vegetation cover was assigned one of the types defined in Table 4 and assumed to be uniform. The reference simulations were chosen as the one leading to the best statistical agreement on the calibration set. The initial fraction of the various vegetation types were: (i),Jarillal: 62% vegetation type 1 and 38% vegetation type 2; (ii), Grande: 68% vegetation type 1 and 32% vegetation type 2; and (iii) Garabato: 76% vegetation type 1 and 24% vegetation type 2

	Reference simulation	Vegetation type 1 Jarillal PER = 0.75	Vegetation type 2 Jarillal PER = 0.52	Vegetation type 1 Grande PER = 0.64	Vegetation type 2 Grande PER = 0.50	Vegetation type 1 Garabato PER = 0.50	Vegetation type 2 Garabato PER = 0.86
Jarillal catchment: reference simulation $DF = 40$ mm $KS = 16$ mm h^{-1}							
B (mm)	− 0.03	− 0.05	− 0.10	− 0.19	0.07	− 0.18	0.20
E (–)	0.39	0.38	0.30	0.31	− 0.07	0.30	− 0.48
RMSE (mm)	0.42	0.42	0.45	0.44	0.55	0.45	0.65
Grande catchment: reference simulation $DF = 150$ mm $KS = 16$ mm h^{-1}							
B (mm)	− 0.02	− 0.06	− 0.01	− 0.05	− 0.01	− 0.01	− 0.06
E (–)	0.60	0.16	0.82	0.44	0.82	0.82	0.18
RMSE (mm)	0.15	0.21	0.10	0.17	0.10	0.10	0.21
Garabato catchment: reference simulation $DF = 150$ mm $KS = 16$ mm h^{-1}							
B (mm)	− 0.11	− 0.19	− 0.12	− 0.18	− 0.13	− 0.11	− 0.19
E (–)	0.60	− 0.17	0.57	0.10	0.53	0.58	− 0.18
RMSE (mm)	0.23	0.39	0.24	0.34	0.25	0.23	0.39

which agrees with the observation. On the other hand, the model calculated a largest runoff on the CAP3 field (42% vegetation cover) than on the CAP2 field (60% vegetation cover), which do not agree with the observations (see Table 8). In this sense, the model was consistent with its own hypotheses, because it calculated a lower effective hydraulic conductivity (taking into account coarse fragments and vegetation cover) for the CAP3 field than for the CAP2 field, which implied that the CAP3 field had a lower infiltration capacity. This parameterization of the model should be improved in order to better fit with observations.

4.2. Application of the ANSWERS model to the three subcatchments (Jarillal, Grande and Garabato)

The best results on the three subcatchments were not obtained with soil characteristics calibrated on the three small plots, except, to a certain extend for the Jarillal catchment. Table 11 and Fig. 10 show the best results. They were poorer than on the three small plots in the calibration phase. Furthermore, they were not stable, as statistics decreased dramatically on the validation samples. Sometimes, negative efficiencies were obtained, which meant that model performance was worse than if observation average had been used as a predictor. It must be kept in mind that a few large events were part of the validation samples and were very badly reproduced by the model. Therefore, a larger sample size, including more large events should be necessary to get more robust results and judge the model more completely. Sediment yield calculated by the model was also compared with observed values. Results were in general poor, in agreement with the poor prediction of runoff. Results are, therefore, not discussed in detail.

Vegetation cover influence on runoff generation was the focus of this study. Sensitivity of model outputs to vegetation cover changes was investigated for each of the sub-catchment. A first set of test was performed assuming uniform vegetation over the whole sub-catchment and the six possible vegetation covers defined for the three sub-catchments (see Table 4) were successively used as uniform vegetation classes. The same statistics, as the ones presented in Table 11 were recalculated in each case. They are given in Table 12 (only for the calibration set). They show that, except for the Grande catchment, better performance were obtained with two vegetation classes on the catchment rather than when using only one of the vegetation type as uniform cover. This

Table 13
Statistical comparison of observed and calculated runoff and peak discharge (1983–1994 period) on the Divisadero Largo catchment. The columns labelled '1983–1990 parameter file' correspond to a use of the 1983–1990 period vegetation characteristics as defined in Section 2.2. The columns labelled '1991–1994 parameter file' correspond to the use of the 1983–1990 vegetation characteristics over the 1983–1990 period and the 1991–1994 vegetation characteristics over the 1991–1994 period

	1983–1990 parameter file		1991–1994 parameter file	
	Runoff volume (mm)	Peak discharge ($m^3 s^{-1}$)	Runoff volume (mm)	Peak discharge ($m^3 s^{-1}$)
B	− 0.01 mm	− 2.45 $m^3 s^{-1}$	− 0.04 mm	− 2.47 $m^3 s^{-1}$
MAE	2.33 mm	5.98 $m^3 s^{-1}$	2.32 mm	5.60 $m^3 s^{-1}$
E	0.615	0.51	0.617	0.513
RMSE	0.62 mm	2.23 $m^3 s^{-1}$	0.62 mm	2.23 $m^3 s^{-1}$
Slope	0.55	0.38	0.54	0.38
Intercept	2.02 mm	4.04 $m^3 s^{-1}$	2.01 mm	4.02 $m^3 s^{-1}$
R^2	0.625	0.625	0.628	0.636

might justify a posteriori the mapping of the vegetation over the catchments. Very bad results were obtained for the Garabato catchment, when the second type of vegetation was supposed to be uniformly distributed over the catchment. This second vegetation type was only covering 24% of the surface.

Three vegetation types were characterized by a vegetation cover of about 50%. However, the surface storage capacities were different due to different stones, mulch and/or gramineas coverage (see Table 5). Despite this difference, statistical results were in general very close for the three corresponding vegetation types, showing that modifications of the surface storage capacity was less influential on model performance than changes in surface cover itself (when surface cover is modified, Leaf Area Index and, therefore, transpiration rates are modified, leading to different initial moisture conditions).

4.3. Application of the ANSWERS model to the Divisadero Largo catchment

Calibration and validation phases of the ANSWERS model had already been reported elsewhere, using a temporally constant vegetation cover (Braud et al., 1999), showing an efficiency of 0.6 for total runoff and 0.46 for peak discharge. The shape of the hydrographs was also satisfactorily reproduced. In this section, it will only be focused on vegetation cover influence on total runoff and peak discharge, using the time evolution of vegetation cover (annual and interannual) described in Section 2.2. Table 13 shows the comparison of the statistical criteria (calculated for the 1983–1994 period with 33 events) listed in Section 2.3 when only one or two vegetation evolution parameter files were considered. Only few differences were obtained between both cases. On the other hand, results were slightly improved as compared to Braud et al. (1999), who used a constant vegetation cover. Peak discharge efficiency was 0.51 instead of 0.46. It showed the interest of taking into account the annual vegetation cover evolution whereas the long term one had no significant impact. Vegetation cover modifications were, therefore, not so influential in the DL catchment as they appeared within the CAP catchment. A first sensitivity analysis performed by Braud et al. (1999) had demonstrated that rainfall and soil type spatial variability were one order of magnitude more influential on runoff generation than vegetation cover spatial variability. This additional study showed that temporal variability of vegetation cover had also little impact on runoff generation. An additional simulation over the 1995–1998 period where no streamflow data were available confirmed these findings. Two simulations were performed: the first one using the 1983–1990 parameter file and the second using the 1995–1998 parameter file (see Section 2.2). 55 events leading to non-zero calculated runoff were selected and statistics of runoff volume and peak discharge compared for the two simulations. This comparison showed a slight decrease in average runoff volume and peak discharge, which did not exceed 2% for runoff and 1% for peak discharge. However, maximum runoff volume was decreased

by 10% and maximum peak discharge by 1% (not shown).

4.4. Discussion

All the results presented in this section and in Braud et al. (1999) showed contrasting performance of the ANSWERS model. It proved to be very well adapted to the simulation of the DL catchment or of the small plots (CAP1, 2, 3), whereas it failed to properly reproduce measured runoff within the sub-catchments of the CAP catchment (Garabato, Grande, Jarillal). Model results were sensitive to vegetation cover within the CAP catchment whereas it has little influence within the DL catchment. Several arguments can explain these results. Within the DL catchment, soil characteristics and rainfall variability appear as the most influential processes on runoff generation, whereas vegetation cover (spatial and temporal variability) is of second order. On the other hand, soil is homogeneous within the CAP catchment. Rainfall variability could be a possible candidate explaining model poor performance within the Jarillal, Grande and Garabato sub-catchments. Rainfall spatial variability is large within the Piemont (cumulative rainfall was found to change by 100% over a few kilometres on the DL catchment for the same event, Braud et al., 1999). Fernández et al. (1999) showed that 10% of a rainfall event falls on less than 5 km^2 and 50% on an area smaller than 100 km^2. In the CAP catchment, the rainfall gauge was situated within 500 m of the various sub-catchments. Variability of cumulative amount other such a short distance should be investigated in order to see if it might be responsible for significant variations of input rainfall over the three sub-catchments.

Another point to be underlined is that it was necessary to adjust soil parameters of the model for all the small plots and sub-catchments in order to reproduce observed runoff and sediment yield. It was not possible to use values adjusted at smaller scales directly at larger scales. These results contrast with those reported by Silburn and Connoly (1995); Connolly and Silburn (1995); Connolly et al. (1997) on agricultural catchments of various sizes in Australia. They calibrated infiltration parameters using rainfall simulator infiltration tests and used the derived values at larger scales with success. The explanation might be a higher homogeneity of agricultural surfaces across scales as compared to natural ones. A possible cause of non-transportability of model calibration from the small plots to the larger scale might be found in the presence of plant-residue mulch and more gramineas at the surface of the catchments than at the surface of the small plots. A more careful vegetation survey, possible preferential infiltration zones and surface storage could perhaps help understanding these differences. Influence of microtopography on runoff has been evidenced in Sahel by Estèves et al. (2000). An accurate definition of this microtopography in relation with vegetation cover could be a research line to investigate further in order to define water paths better. Such a study could invalidate the modelling of surface runoff as homogeneous plane surfaces.

5. Summary and conclusions

In this study, the ANSWERS model was applied in the Andes region of Mendoza at three scales: the local scale (30–50 m^2), the slope scale (0.2–0.5 ha) and the small catchment scale (5.47 km^2). The focus was on vegetation cover influence on runoff and sediment yield generation, the various catchments exhibiting different vegetation coverage. This study also enabled us to judge the possibility of using the same model across scales.

A first part of the study was dedicated to the mapping of vegetation cover and the definition of its time evolution. For the smallest scales, in situ measurements were used and are relatively easy to implement. For larger scales, such a global survey becomes impossible. The problem was addressed through satellite image analysis. A methodology was proposed in order to define vegetation cover maps from Landsat TM3 and 4 channels and a limited number of in situ measurements. The long term evolution of the vegetation cover (difference between pre and post-closure cover) as well as seasonal evolution were correctly seen. About three to four images per year could be sufficient to define this seasonal evolution correctly.

Application of the same model across scales showed contrasting results. The ANSWERS model seems to be well adapted when soil variability (and especially quite impervious regions can be identified)

and rainfall variability are the dominant processes explaining runoff generation. However, when the microtopography of the surface and vegetation cover might be the dominant process explaining runoff paths, the model fails to correctly reproduce measurements. A much finer resolution of topography would be needed in order to identify water paths better. This would imply a different modelling of overland flow, water movement over plane sheets being invalidated in this case. A better representation of vegetation and surface feature in the parameterization of infiltration would also be needed, because the actual one fails to reproduce differences in behaviours observed in the field. It would remain to validate these hypotheses, once the question of rainfall variability at small scales (of the order of 100 m) has been resolved in this region, using appropriate rainfall gauges sampling.

Acknowledgements

This study was funded by the Centre National de la Recherche Scientifique (CNRS), through a grant allocated to the first author for an 8-month stay at INA-CRA, Mendoza. Faycal Bouraoui is especially thanked for providing the ANSWERS model code used in this study.

References

Beasley, D.B., Huggins, F., Monke, E.J., 1980. ANSWERS: a model for watershed planning. Trans. of the ASAE 23 (4), 938–944.

Bergkamp, G., 1998. A hierarchical view of the interactions of runoff and infiltration with vegetation and micotopography in semiarid shrublands. Catena 33, 201–220.

Bouraoui, F., Dillaha, T.A., 1996. ANSWERS 2000: runoff and sediment transport model. J. Environ. Eng. 122, 493–502.

Bouraoui, F., 1994. Development of a continuous, physically-based distributed parameter, nonpoint source model, PhD Thesis, Virginia Polytechnic Institute and State University, Blacksburg, VA.

Bouraoui, F., Braud, I., Dillaha, T.A., 2000. ANSWERS: a non-point source pollution model for water, sediment and nutrient losses. In: Frevert, D., Meyer, S., Singh, V. (Eds.). Mathematical Models of Watershed Hydrology. Water Resources Publications, Littleton, CO.

Bras, R.L., 1990. Hydrology: an introduction to hydrological sciences. Addison-Wesley Publishing Company, Addison-Wesley series in Civil Engineering.

Braud, I., 1999. Hydrological studies using remote sensing and GIS in the region of Mendoza (Argentina)—study of vegetation cover influence on runoff and sediment yield. Activity report 01/11/98 to 30/06/99. Available from LTHE, BP 53, 38041 Grenoble Cedex 9, France.

Braud, I., Fernández, P.C., Bouraoui, F., 1999. Study of the rainfall–runoff process in the Andes region using a continuous distributed model. J. Hydrology 216, 155–171.

Connolly, R.D., Ciesiolka, C.A., Silburn, D.M., Carroll, C., 1997. Distributed parameter hydrology model (ANSWERS) applied to a range of catchment scales using rainfall simulator data. IV Evaluating pasture catchment hydrology. J. Hydrology 201, 311–328.

Connolly, R.D., Silburn, D.M., 1995. Distributed parameter hydrology model (ANSWERS) applied to a range of catchment scales using rainfall simulator data. II: application to spatially uniform catchments. J. Hydrology 172, 105–125.

Descroix, L., Nouvelot, J.F., 1997. Escurrimiento y erosion en la Sierra Madre Occidental, INIFAP-ORSTOM, Folleto Cientifico no. 7, CENID-RASPA, Mexico.

Descroix, L., Viramontes, D., Vauclin, M., Gonzalez Barrios, J.L., Estèves, M., 2001. Influence of soil surface features and vegetation on runoff and erosion in the Western Sierra Madre (Durango, Northwest Mexico). Catena 43, 115–135.

Eastman, J.R., 1995. IDRISI for Windows User's guide, version 1.0., Clark Labs for Cartographic Technology and Geographic Analysis, Clark University, MA.

Estèves, M., Faucher, X., Galle, S., Vauclin, M., 2000. Overland flow and infiltration modelling for small plots during unsteady rain: numerical results versus observed values. J. Hydrology 228, 265–282.

Fernández, P.C., Roby, H.O., Tarantola, D., 1988. Sistema de alerta hidrologica aluvional: 6 años de experiencia. INCyTH-CRA, Mendoza, Argentina.

Fernández, P.C., Fattorelli, S., Rodríguez, S., Fornero, L., 1999. Regional analysis of convective storms. J. Hydrologic Engineering, ASCE 4 (4), 317–325.

Foster, G.R., 1976. Sedimentation, general. Proceedings of the National Symposium on Urban Hydrology, Hydraulics and Sediment control, University of Kentucky, Lexington, KY, 129–138.

Green, W.H., Ampt, G.A., 1911. Studies on soil physics. J. Agric. Sci. 4, 1–24.

Horton, R.E., 1940. An approach towards a physical interpretation of infiltration capacity. Soil Sci. Soc. Am. Proc. 5, 399–417.

Ligtenberg, A., van Rijswijk, J., Menenti, M., Fernández, P., 1992. Runoff Research 'Divisadero Largo': an attempt to calibrate the soil water model SWAMIN for a catchment in the Andean Precordillera. The Winand Staring Center, Wageningen, The Netherlands.

Mantz, P.A., 1977. Incipient transport of fine grains and flakes by fluids-extended Shield's diagram. Journal of Hydraulic division, Proceedings of the ASAE 103 (HY6), 601–615.

Meyer, L.D., Wischmeier, W.H., 1969. Mathematical simulation of the processes of soil erosion by water. Transactions of the ASAE 12 (6), 754–758.

Nave, M.R., 1996. Análisis de la infiltración y su relación con los modelos de lluvia-caudal y con el manejo de cuenca, informe de

avance, beca de perfeccionamiento. Centro Regional de Investigaciones Cientificas y Tecnicas (CRICYT), Mendoza, Argentina.

Ritchie, J.T., 1972. A model for predicting evapotranspiration from a row crop with incomplete cover. Water Resour. Res. 8 (5), 1204–1213.

Roby, O., Maza, J., Zuluaga, J., Fornero, L., 1988. Determinación de parametros para modelos hydrologicos con sensores remotos. In: Menenti, M. (Ed.). Mecanismos de aprovechamiento hidrico en la región Andian. Modelos de simulación e imagenes satelitarias. ICW, INCYTH, CRICYT, DGI, Mendoza, Argentina, pp. 55–67.

Silburn, D.M., Connolly, R.D., 1995. Distributed parameter hydrology model (ANSWERS) applied to a range of catchment scales using rainfall simulator data. I:Infiltration modelling and parameter measurement. J. Hydrology 172, 87–104.

Van Deursen, W.P.A., Wesseling, C., 1992. The PC RASTER package, Department of Physical Geography, The University of Utrecht, The Netherlands.

Vich, A.I.J., 1996. Aguas continentals. Formas y procesos, Departamento de Geografia, Facultad de Filosofia y Letras, Universidad Nacional de Cuyo, Argentina, impimido por el CELAA.

Vich, A., Mariani, A., Pedrani, A., 1998. Evaluación y predicción de la erosión hídrica en regiones áridas de relieve acentuado. Congreso Nacional del Agua, Santa Fe, Argentina, 3–7/08/98. pp. 297–306.

Vich, A., Nave, M., 1998. Ajuste de modelos de infiltración en suelos poco evolucionados. Congreso Nacional del Agua, Santa Fe, Argentina, 3–7/08/98. pp. 33–43.

Wischmeier, W.H., Smith, D.D., 1978. Predicting rainfall erosion losses—a guide to conservation planning, Agriculture Handbook 537, Science and Education Administration, US Department of Agriculture.

Yalin, Y.S., 1963. An expression for bed-load transportation. Journal of Hydraulics Division, Proceedings of the ASAE 89 (HY3), 221–250.

Zuluaga, J., Basile, J.C., Collado, D., 1988. Censo de cultivos e identificación de viñedos abandonandos y erradicados. In: Menenti, M. (Ed.). Mecanismos de aprovechamiento hidrico en la región Andian. Modelos de simulación e imagenes satelitarias. ICW, INCYTH, CRICYT, DGI, Mendoza, Argentina, pp. 205–225.